

RESEARCH ARTICLE

Inhibitory Effects of Novel SphK2 Inhibitors on Migration of Cancer Cells

Euiyeon Lee¹, Junghyun Jung², Deokho Jung¹, Chang Soo Mok², Hyunjin Jeon¹, Chang-Seo Park³, Wonhee Jang^{2,*} and Youngeun Kwon^{1,*}

¹Department of Biomedical Engineering; ²Department of Life Science; ³Department of Chemical Biological Engineering, Dongguk University, Pildong 3-ga, Seoul, Korea 04620

Abstract: Background: Cell migration is an essential process for survival and differentiation of mammalian cells. Numerous diseases are induced or influenced by inappropriate regulation of cell migration, which plays a key role in cancer cell metastasis. In fact, very few anti-metastasis drugs are available on the market. SphKs are enzymes that convert sphingosine to sphingosine-1-phosphate (S1P) and are known to control various cellular functions, including migration of cells. In human, SphK2 is known to promote apoptosis, suppresses cell growth, and controls cell migration; in addition, the specific ablation of SphK2 activity was reported to inhibit cancer cell metastasis.

ARTICLE HISTORY

Received: June 03, 2016
Revised: December 12, 2016
Accepted: February 03, 2017

DOI:
10.2174/18715206176661702131248
56

Objective: The previously identified SG12 and SG14 are synthetic analogs of sphingoid and can specifically inhibit the functions of SphK2. We investigated the effects of the SphK2 specific inhibitors on the migratory behavior of cells.

Method: We investigated how SG12 and SG14 affect cell migration by monitoring both cumulative and individual cell migration behavior using HeLa cells.

Results: SG12 and SG14 mutually showed stronger inhibitory effects with less cytotoxicity compared with a general SphK inhibitor, N,N-dimethylsphingosine (DMS). The mechanistic aspects of specific SphK2 inhibition were studied by examining actin filamentation and the expression levels of motility-related genes.

Conclusion: The data revealed that SG12 and SG14 resemble DMS in decreasing overall cell motility, but differ in that they differentially affect motility parameters and motility-related signal transduction pathways and therefore actin polymerization, which are not altered by DMS. Our findings show that SphK2 inhibitors are putative candidates for anti-metastatic drugs.

Keywords: Anti-metastasis, motility parameters, SphK2-specific inhibitors, sphingosine analogues, migration inhibitors, cancer therapeutics.

1. INTRODUCTION

Cell migration is an essential process for the survival and development of multicellular organisms and also plays a key role in wound repair and immune surveillance. A number of diseases, including cancer, are induced or influenced by inappropriate regulation of cell migration. One of the key features in cancer progression is metastasis, which is closely related to cell migration. Migration of cells is often directly cued by extracellular signals, which may act either as a stimulator or an inhibitor, and understanding how these factors modulate cell migration and identifying effectors involved in the processes provides an important first step in developing new drug candidates for various diseases.

Sphingosine kinases (SphKs) are important regulators of various cellular functions including cell division, growth, differentiation, migration, immune response, and apoptosis [1]. SphKs convert sphingosine to sphingosine-1-phosphate (S1P), and these bioactive sphingolipids act as signaling molecules in the above-mentioned cellular processes. Two isozymes of SphKs (SphK1 and SphK2) have been identified in humans so far, and they play different roles. Generally, SphK1 promotes cells growth and survival in various cell types, while SphK2 promotes apoptosis and suppresses cell growth. Reports also indicated that the specific ablation of SphK2

activity inhibited cancer cell proliferation as well as migration and that SphK2-specific inhibitors showed anti-tumor activity in mouse models [2, 3]. Since SphK2 modulates cell migration, we decided to investigate the effects of previously identified SphK2-specific inhibitors on migratory events of cells.

Among 16 previously synthesized analogs of sphingoid (SG1-SG16) [4], SG12 and SG14 were identified as specific inhibitors for SphK2 without notable inhibitory effects on SphK1 (Fig. 1A). As SphK1 is known to mainly regulate cell growth and survival, we expected SphK2-specific inhibitors to affect cell migration without significant interference on cell survival. N,N-Dimethylsphingosine (DMS) is a potent non-specific inhibitor for both SphK1 and SphK2, as well as for protein kinase C (PKC). DMS is often cytotoxic and induces cell death in various cell types, as it affects vital signal pathways of cellular functions [5]. Thus, we hypothesized that specific inhibition of SphK2 may mainly alter migratory behavior with minimal effects on cell growth and survival.

Here, we investigated the effects of SphK2-specific inhibitors on cell migration by monitoring cumulative behaviors of cells using a gap filling assay and individual behaviors of cells using computer-aided motility analysis. The rearrangement of actin cytoskeleton due to the treatment of SphK2 inhibitors was monitored, and the expression levels of motility-related pathway genes were determined. The results suggest that anti-migratory effects of SphK2-specific inhibitors can be employed in developing novel anti-metastatic drug candidates.

*Address correspondence to these authors at the Department of Lifescience; Tel: +82-32-961-5134; E-mail: wany@dongguk.edu and Department of Biomedical Engineering, College of Biosystems, Dongguk University, Seoul, Korea; Tel: +82-32-961-5151; E-mail: ykwon@dongguk.edu

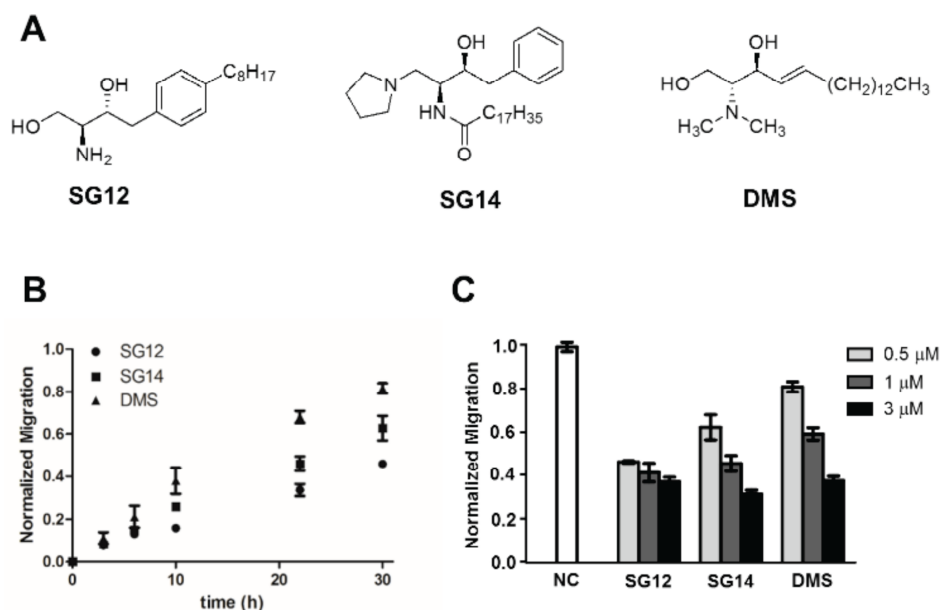


Fig. (1). Structures of SphK inhibitors and their effects on cumulative migration in mammalian cells. (A) Structures of sphingosine kinase inhibitors. (B) The effects of SphK2 inhibitors on cell motility. The effects of SphK2 inhibitors were studied by monitoring the cumulative migratory behaviors of HeLa cells after the treatment of 0.5 μM of each inhibitor based on a gap filling assay. The migration distance was measured and normalized against non-treated HeLa cells at each time point. SG12 showed the most effective inhibitory effect at the concentration used. (C) Normalized cell motility after treatment of SphK2 inhibitors of varying concentrations. The inhibitory effect of each inhibitor on the cumulative migration was studied using varying concentrations of inhibitors. All inhibitors showed comparable inhibition at concentrations higher than 1 μM .

2. MATERIALS AND METHOD

2.1. Cell Culture

HeLa cells were cultured in Dulbecco's modified Eagle's medium (DMEM) supplemented with 10% fetal bovine serum (FBS), and antibiotics (streptomycin, penicillin) at 37°C in a humidified atmosphere composed of 5% CO_2 and 95% air. All experiments were performed in a plastic 12-well plate. Each well was coated with fibronectin solution (10 $\mu\text{g}/\text{ml}$ in PBS) for 1 h before seeding cells (2.1×10^4 cells/ cm^2). Cells were counted before seeding using an ADAM automated cell counter (Labtech International Ltd.).

2.2. Gap Filling Assay

Gap filling assay was performed to monitor collective migration of cells *in vitro*. Regular-shaped capillaries were placed in the fibronectin coated wells of 12-well plates (Corning Inc.). Then, 8×10^4 cells were plated onto the 12-well plate with a capillary and grown to near confluence in DMEM containing 10% FBS and 1% penicillin and streptomycin. The capillary was removed once cells adhered to the substrate and the culture media was replaced to DMEM containing 1% FBS. Target inhibitor, SG12, SG14, or DMS, was added to each well containing a monolayer of cells with regular-sized gaps, and cells were incubated continuously for 36 h. The gap distance was observed by phase contrast microscopy (Nikon) at time 0 and every few hours up to 36 h. The distance of the open gap was measured by NIS Elements Version 3.22 (Nikon). Two independent experiments were performed with each in triplicate. The migration distance was normalized using the non-treated negative control.

2.3. Computer-aided Cell Migration Analysis

HeLa cells were seeded at 2.6×10^3 cells/ cm^2 in a 12-well plate and incubated for 12 h. A cell density was determined that allowed individual, uninterrupted cell migration over an 11 h period, during

which time cells were imaged through a bright-field 10x objective. Then, each well was treated with 1 μM SG12, SG14, or DMS, respectively. For a negative control, cells were treated with medium only. Time-lapse images were generated using NIS Elements Version 3.22 at 20 min intervals, and then exported into ImageJ 1.45s/Java 1.6.0_20 (<http://rsb.info.nih.gov/ij/>). Using a total of 454 cells (Negative: 136, SG12: 70, SG14: 143, DMS: 105) from at least four independent assays, motility parameters were computed from the centroid positions and dynamic morphology parameters such as speed, acceleration, persistence, direction change, and trajectories from contours of the replacement images following Soll and Wessels (1998). Any cells that are touching other cells were eliminated from the count because their normal behaviors were considered to be hindered. In addition, cells that moved less than 20 μm for the duration of 11 h were eliminated from the count, considering them to be non-motile unhealthy cells, as it falls within the margin of error in calculating the centroid from an approximately 100 μm -diameter cell between frames. The related formula for distribution change (θ_{dirch}) is given below (eq. 1):

$$\Delta\theta = \frac{180}{\pi} \left[\text{atan}\left(\frac{y_3}{x_3}\right) - 2 \text{atan}\left(\frac{y_2}{x_2}\right) + \text{atan}\left(\frac{y_1}{x_1}\right) \right] \quad (\text{Eq. 1})$$

$$\theta_{dirch} = \begin{cases} \text{abs}(\Delta\theta), & -180 \leq \Delta\theta \leq 180 \\ 360 - \text{abs}(\Delta\theta), & \text{otherwise} \end{cases}$$

The persistence (eq. 2) was also calculated *via* dividing the speed by the direction change for frame by frame. The integer 1 is added to make a non-zero denominator for non-turning cells, which have θ_{dirch} of zero. The persistence becomes the same as the speed for those non-turning cells in this equation. The related formula for calculating persistence is given below (eq. 2):

$$\text{Persistence} = \frac{\text{speed}}{1 + \frac{100}{360} \theta_{dirch}} \quad (\text{Eq. 2})$$

2.4. F-actin Staining

HeLa cells were plated on cover glass at a density of 1×10^4 cells/cm² and allowed to grow at 37°C with 5% CO₂ for 12 h. Twelve hours after seeding, complete culture medium was replaced with 1% FBS containing media, and cells were treated with 1 and 3 μM of SG12 and SG14, or DMS for 30 h. At the end of the exposure time, the cells were fixed with 3.7% (v/v) formaldehyde and stained with the Alexa Fluor[®] 568 phalloidin (Invitrogen, CA, USA) and DAPI to visualize the actin and the nucleus, respectively. The cover slides were mounted in slide glass, and images were taken using an Eclipse Ti confocal laser scanning microscope (Nikon Instruments, Ontario, Canada) to observe any morphological changes. The stress fibers were quantified using ImageJ software. Ten cells were randomly selected in each group from images of confocal microscopy, and then the images were converted into 8-bit grey scale. Spreading area of the cells was calculated by Auto threshold using Intermodes method [6]. Subsequently, the number of stress fibers was quantified using ImageJ plugin, Ridge Detection (Sigma = 1.5, Lower Threshold = 2.5, Higher Threshold = 5) [7].

2.5. RNA Extraction

HeLa cells (1.2×10^6) treated with each inhibitor for 11 h were resuspended in 1 ml TRIzol reagent (Invitrogen, Madison, USA). Chloroform (200 μl) was added, followed by vigorous shaking and centrifugation for 15 min at 12,000 x g and 4°C. The upper aqueous layer was placed in a new tube, and 500 μl isopropanol was added and incubated at room temperature for 10 min, followed by centrifugation for 15 min at 12,000 x g and 4°C. The RNA pellet was washed once with 75% ethanol and was dissolved in diethylpyrocarbonate-treated water.

2.6. Reverse Transcription and RT-PCR

To synthesize cDNA for RT-PCR, RNA was quantified and DNase was treated with RQ1 RNase-free DNase kit (Promega, Madison, USA) to remove contaminating genomic DNA. Then, 1 μg RNA was reverse-transcribed using the Reverse Transcription System (Promega) according to the manufacturer's instructions with oligo-dT primer. Briefly, 1 μg RNA was incubated at 70°C for 10 min and then placed on ice for 5 min. For the reverse transcription reaction, 5 mM MgCl₂, 1X Reverse Transcription Buffer, 1 mM dNTP Mixture, 20 unit Recombination RNasin Ribonuclease Inhibitor (Promega, Madison, USA), 15 unit AMV Reverse Transcriptase, and 0.5 μg Oligo-dT Primer were mixed with the 1 μg RNA and incubated at 45°C for 1 h, followed by inactivation at 95°C for 5min, and then placed on ice for 5 min. PCR was performed in a 20 μl reaction volume that was composed of 1X KAPA2G[™] Hotstart ReadyMix (Kapabiosystems Wilmington, USA) with 500 nM of each target-specific forward and reverse primer and 200 ng cDNA as template. Target genes and specific primer pairs are listed in Table S1. *GAPDH* was used as an internal control for relative gene quantification. Amplification conditions were 95°C for 3 min, followed by 35 cycles of 95°C for 30 s, 60.5°C for 30 s, and 72°C for 30 s. MyCycler[™] Personal Thermal Cycler (Bio-Rad, Hercules, USA) was used for thermal cycling reaction. PCR products were separated by gel electrophoresis on 1.2% agarose gels with ethidium bromide staining, and images were obtained by using the Clinx GenoSens gel documentation system (Clinx Science Instruments, Shanghai, China), followed by quantifying the RT-PCR bands using NIH ImageJ image analysis software (National Institutes of Health, Bethesda, USA). Each gene was normalized against *GAPDH* as a housekeeping gene control. A representative result from at least 7 independent experiments was shown.

2.7. Heatmap Generation and Gene Regulation Analysis

Heatmaps were generated from the quantified RT-PCR data using the *heatmap* package in R (version 3.2.2). The expression levels were normalized by using GAPDH as an internal control, and then each value was normalized against the no treatment control in order to identify fold change of motility-related genes. Up- and down-regulated genes were selected by applying a minimal 2-fold change as cut-off. The clustering columns and rows were based on both Euclidean distance and complete linkage method.

2.8. Pull-down Assays

Pull-down assays of active RhoA and Cdc42 were performed using the activity assay kit purchased from Cytoskeleton (Denver, CO, USA). The assays were performed after 30 min exposure of cells to each inhibitor following the manufacturer's suggestion.

2.9. Statistics

All statistics were done with Prism 5 (GraphPad software, San Diego, CA). Comparisons between groups were made by one-way ANOVA followed by Dunnett's multiple comparison test as post-test and by one-tailed t-test, where indicated. Significance was defined as $P < 0.05$.

3. RESULTS

3.1. Effects of SG12 and SG14 on Cell Viability

We first determined the cytotoxicity of SG12, SG14, and DMS by MTT ((3-(4,5-Dimethylthiazol-2-yl)-2,5-diphenyltetrazolium bromide) assays. The chemical structures of SG12, SG14, and DMS are shown in Fig. 1A. HeLa cells were chosen, as they have been widely tested for various cell-based assays and, thus, have a large set of data for comparison. HeLa cells were treated with SG12, SG14, or DMS at a series of concentrations from 0.5 μM to 30 μM for 30 h, and the dose response curves were obtained (Fig. S1). The observed LD₅₀'s were 6.0 μM, 4.7 μM, and 2.9 μM for SG12, SG14, and DMS, respectively. A nonspecific inhibitor, DMS, was more cytotoxic than SphK2 inhibitors, SG12 and S14, which did not exhibit significant loss of cell viability up to 3 μM.

3.2. Effects of SG12 and SG14 on Cumulative Cell Motility

In order to understand the effects of the three inhibitors on cumulative cell migration, we designed a gap filling assay. Gaps between cell patches are usually generated by scratching cell patches with a sharp object. However, creating a gap by scratch in the laboratory suffers from reproducibility and consistency issues, as it is difficult to create an identical scratch area every time. Scratching may also damage the extracellular matrix between cells and the substratum as well as cells directly touching the scratch site, which may lead to an imprecise measurement [8]. In order to address these limitations, we generated an evenly sized gap without peeling off the surface fibronectin coating by placing a glass capillary in a well before cells were plated. After cells were seeded, adhered to the surface, and grown to near confluence, the capillary was removed to reveal an evenly sized gap with well-maintained homogenous fibronectin coating.

Cells were then treated with varying concentrations (0.5–3 μM) of SG12, SG14, and DMS, respectively, in 1% FBS-supplemented medium to minimize proliferation. The size of the gap was measured by phase-contrast microscopy up to 30 h, and the migration rate was normalized against non-treated cells. The rates of cell migration were lower in all three inhibitor-treated groups compared with the negative control and decreased as the concentrations of inhibitors increased (Fig. 1B). At a concentration

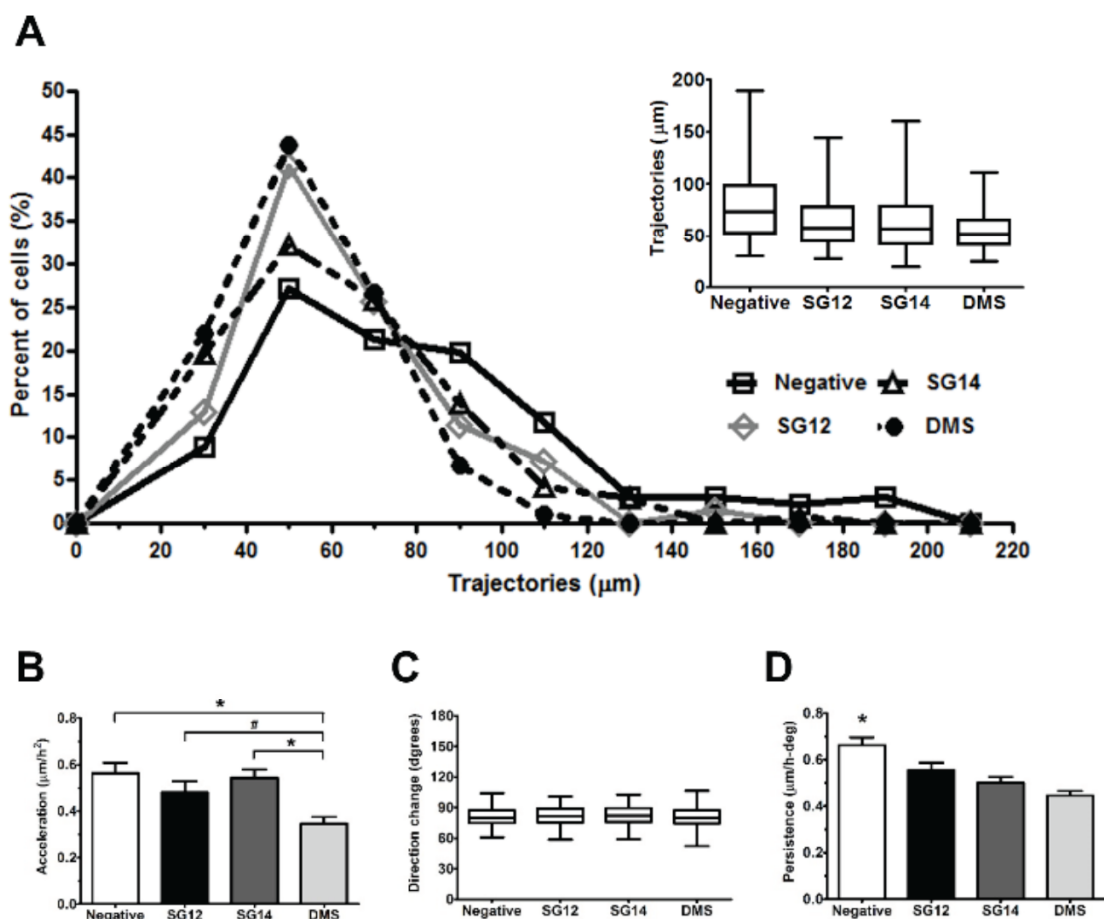


Fig. (2). Individual cell motility analysis. The motility analysis of a total of 454 cells (Negative: 136, SG12: 70, SG14: 143, DMS: 105) treated with different drugs (SG12, SG14, DMS) migrated over 11 hours were observed using time-lapse videomicroscopy with 20-minute intervals. (A) The distribution of trajectories under different treatments and additional boxplot insets. (B) The average acceleration of cells under different treatments. (C) The distribution of direction change in cells under different treatments. (D) The average persistence of cells under different treatments. The error bars for all graphs indicate means \pm SEM. * and # indicate significant difference ($P < 0.05$) using one-way ANOVA with Dunnett's multiple comparison test as post-test or one-tailed t-test, respectively.

of 0.5 μM , SG12 showed the most efficient inhibition of migration, followed by SG14. DMS was the least effective on inhibiting migration of cells at 0.5 μM . While 1–3 μM DMS-treated cells showed an apparent retardation of 40–50% on the migration rate, we also observed substantial cell death, suggesting that the observed delay in gap filling may partly be due to the reduced number of viable cells, not solely due to the actual inhibition of cell migration *per se*. Cell migration was monitored at varying time points after the addition of 0.5 μM inhibitors. SG12-treated cells showed the slowest migration at all time-points (Fig. 1C). Together, the data suggest that SG12 and SG14 inhibit the cell migration more efficiently compared with a non-specific inhibitor, DMS, at a low concentration (0.5 μM) and that all three inhibitors, nonetheless, show similar inhibitory effects at a high concentration (3 μM) due to the actual inhibition and/or cytotoxicity. The SG12, SG14, and DMS also inhibited the migration of non-cancerous NIH 3T3 cells. However, the degree of inhibition was smaller and the effects of the three inhibitors were similar in non-cancerous cells (data not shown).

3.3. Effects of SG12 and SG14 on Individual Motility Parameters

Because cumulative cell motility is a complex end-result of different motility parameters, we tried to understand how various motility parameters are affected in individual cells upon the treatment of each inhibitor. HeLa cells were treated with 1 μM

SG12, SG14, or DMS, respectively, and the migratory behavior was observed using time-lapse videomicroscopy for 11 h. The concentration of inhibitors was chosen such that the effects of the three inhibitors were similar in the gap filling experiment (Fig. 1C). All the experiments were performed using 12-well plates coated with fibronectin in order to mimic the extracellular matrix of mammalian cells for effective cell adhesion to the plate and optimal migration behavior.

The trajectory of each cell migrated during 11 h with intervals of 20 min was analyzed using ImageJ (Fig. 2A). The graph showed that treating cells with SG12, SG14, or DMS decreased cell trajectory compared with the negative control by positively skewing the overall cell motility. For the duration of monitoring, cells that migrated over 100 μm were 8.6%, 7.7%, or 0.9% in cells treated with SG12, SG14, or DMS, respectively, whereas control cells migrated over 100 μm were 22.8%. The data suggest that the number of faster migrating cells was significantly reduced by the treatment of the inhibitors (Chi-squared test, $P < 0.05$). The distribution of the trajectory of each group is shown as an inset in



The boxplot of trajectories also showed that the cell motility increased by SG12, SG14, or DMS treatments. The median trajectories of SG12-, SG14-, or DMS-treated cells were 57.89 μm , 56.81 μm , or 51.74 μm , respectively, which were substantially smaller compared with the negative control (73.32 μm). Moreover, the data showed that the negative control cells had the widest range

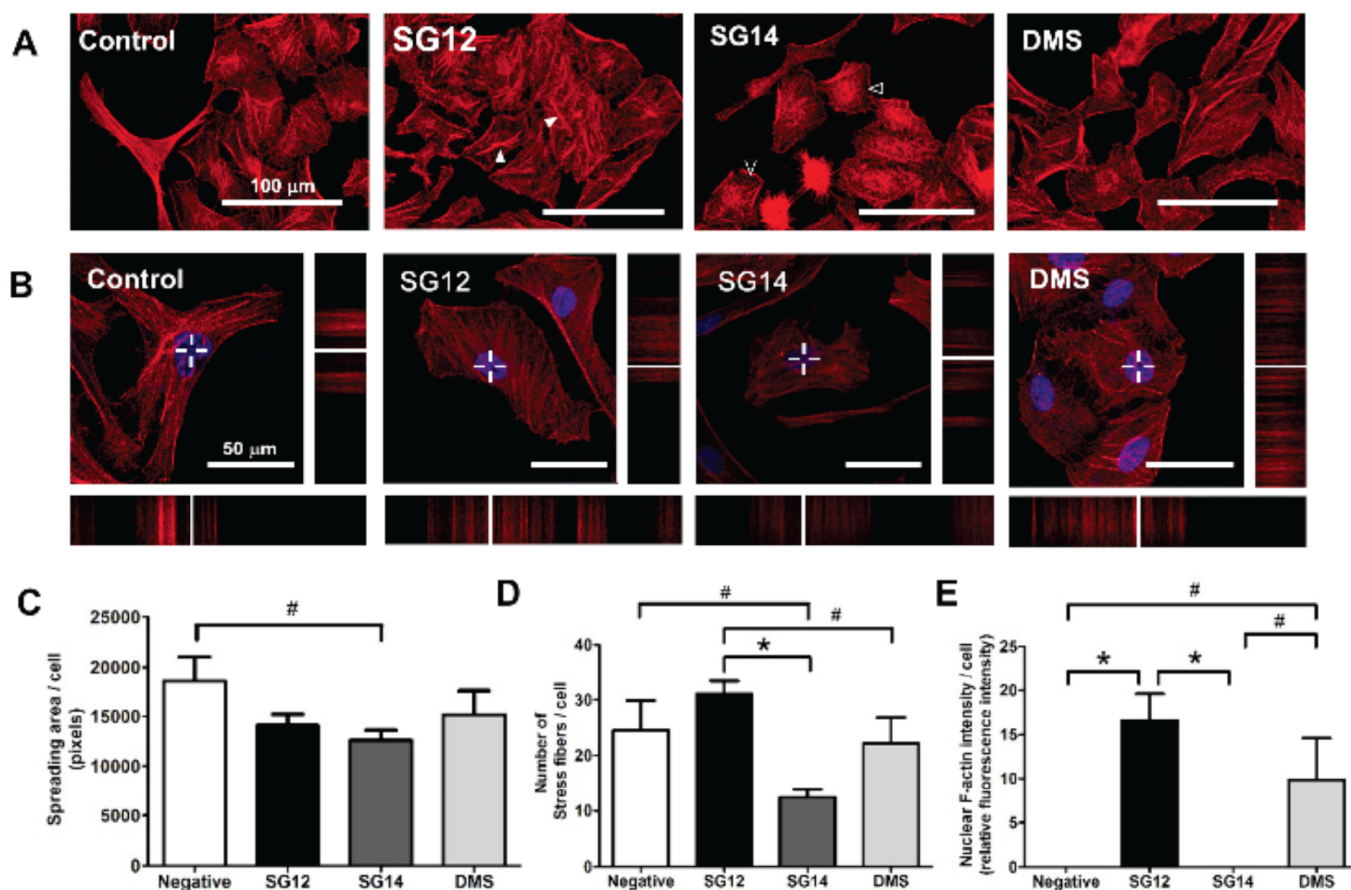


Fig. (3). F-actin and nuclear F-actin staining. (A) The F-actin cytoskeletal structure of cells treated with different drugs (SG12, SG14, DMS). Actin filaments were analyzed by confocal microscopy. The scale bars indicate 100 μm . (B) Nuclear F-actin staining of different inhibitor-treated cells using confocal microscopy. Right panels and bottom panels indicate z-stacked images of optically sectioned cells, with white lines indicating the cross-sectional planes. Actin filaments are shown in red, and nuclei are counter stained with DAPI (blue). Arrow heads indicate heavy stress fiber formation, and open arrow heads indicate the absence of F-actin staining. The scale bars indicate 50 μm . (C) The spreading area of cells. (D) The number of stress fiber per cell. (E) The intensity of nuclear F-actin per nucleus. The values represent means \pm SEM from at least 4 independent experiments. * and # indicate significant difference ($P < 0.05$) using one-way ANOVA with Dunnett's multiple comparison test as post-test or one-tailed t-test, respectively.

of trajectories with the longest upper whisker, suggesting that there are more fast-moving cells compared with inhibitor-treated cells. Together, the trajectory analysis suggests that these inhibitors may decrease cell motility by specifically targeting fast-moving cells. As for acceleration, DMS-treated cells had clearly lower value compared with other three groups. Even though it was not statistically significant, we also repeatedly observed a trend that the acceleration of SG12-treated cells was lower than that of control cells. In short, treating cells with specific and non-specific inhibitors of SphK2 modulated acceleration, cell speed, and thereby persistence, but not direction change.

The average speed (trajectory/h, means \pm SEM) of cells treated with SG12, SG14, or DMS was $5.59 \pm 0.25 \mu\text{m/h}$, $5.48 \pm 0.19 \mu\text{m/h}$, or $4.80 \pm 0.14 \mu\text{m/h}$, respectively, which was significantly slower compared with the negative control ($6.98 \pm 0.27 \mu\text{m/h}$) ($P < 0.05$). In contrast, the average acceleration (trajectory/h², means \pm SEM) of cells treated with SG12, SG14, DMS, or negative control was $0.48 \pm 0.05 \mu\text{m/h}^2$, $0.54 \pm 0.04 \mu\text{m/h}^2$, $0.35 \pm 0.03 \mu\text{m/h}^2$, or $0.56 \pm 0.04 \mu\text{m/h}^2$, respectively (Fig. 2B). Although the acceleration of cells treated with SG12 or SG14 was not significantly decreased when compared with the control, cells treated with DMS showed a significantly decreased acceleration from the control ($P < 0.05$). The distribution of direction change of cells per frame (θ_{dirch}) showed that cells treated with the three inhibitors of migration had middle 50% values and spreads similar

to the negative control (Fig. 2C), suggesting that the inhibitors did not affect the direction changes of cells. The average persistence ($\mu\text{m/h-deg}$, means \pm SEM) of cells, which is an indicator of whether cells are persistently migrating in one direction or in a "jittery" manner, treated with SG12, SG14, or DMS was $0.55 \pm 0.03 \mu\text{m/h-deg}$, $0.50 \pm 0.02 \mu\text{m/h-deg}$, or $0.45 \pm 0.02 \mu\text{m/h-deg}$, respectively, while negative control cells had a higher average persistence of $0.66 \pm 0.03 \mu\text{m/h-deg}$ (Fig. 2D). The difference in average persistence between SG12- and SG14-treated cells were not statistically significant by one-way ANOVA with Dunnett's multiple comparison test as post-test. However, one-tailed t-test suggested that they were marginally different ($P < 0.1$).

The assessment of the individual motility parameter shows that the observed retardation result in gap filling assay could not simply be explained by one parameter such as average speed, trajectories direction changes, or acceleration, but rather by combined effects of the parameters.

3.4. Effects of SG12 and SG14 on Cytoskeletal Structures

In order to understand the mechanistic aspects of migration inhibition, we monitored the changes in cell morphology as well as cytoskeletal structures after the treatment of each inhibitor. As temporal and spatial regulation of actin polymerization plays a major role in cell motility, we examined the differential arrangements of actin by staining filamentous actin (F-actin) with

fluorophore-conjugated phalloidin, which was visualized by fluorescent microscopy (Fig. 3A).

In terms of cell morphology change, the inhibitor-treated cells lost major characteristics of motile cells such as polarized morphology, whereas control cells had well-defined lamellipodia with extensive filopodia and long F-actin formation. DMS-treated cells had similar spreading area and similar number of stress fibers compared with control groups and showed a decrease in filopodia formation (Fig. 3B). SG12-treated cells had less frequency of severely polarized cells, and the periphery of SG14-treated cells had reduced filopodia formation and increased ruffled edges and often appeared grainy, probably due to the formation of short F-actin. The size of spreading area was decreased in SG12- and SG14-treated cells compared with control cells ($P < 0.06$ and $P < 0.05$ using one-tailed t-test) (Fig. 3C).

While the inhibitor-treated cells commonly lost the polarized morphology, the cytoskeletal structures changed in different manners which are specific to each inhibitor. F-actin can form higher-order structures such as stress fibers and nuclear F-actin to control cell migration as well as morphology-related lamellipodia

and filopodia [9]. Stress fibers are implicated in the contractility of motile cells, thereby promoting cell migration. SG14-treated cells had significantly decreased stress fibers and long F-actin formation compared with control ($P < 0.05$) (Fig. 3D and 3E).

Previous works showed that nuclear F-actin forms during cell adhesion and spreading and that cells with nuclear F-actin staining are spread out, less polarized, and, therefore, less motile [10]. In most cells from the four groups, we observed F-actin staining localized near the nucleus. In order to determine whether the near-nuclear F-actin is formed within or on the periphery of the nucleus, we compiled z-stack images of longitudinal and equatorial optical sections of cells stained with both DAPI and F-actin (Fig. 3B and 3E). Cross-sectional planes are shown as lines in Fig. 3B. The reconstructed Z-stack images showed that even though F-actin staining co-localized with the nucleus in every group. All the observed SG12-treated cells showed internal nuclear F-actin staining, whereas an approximately 50% of DMS-treated cells had nuclear F-actin staining.

Together, these results show that the three inhibitors alter cytoskeletal structure in different manners. We infer that the

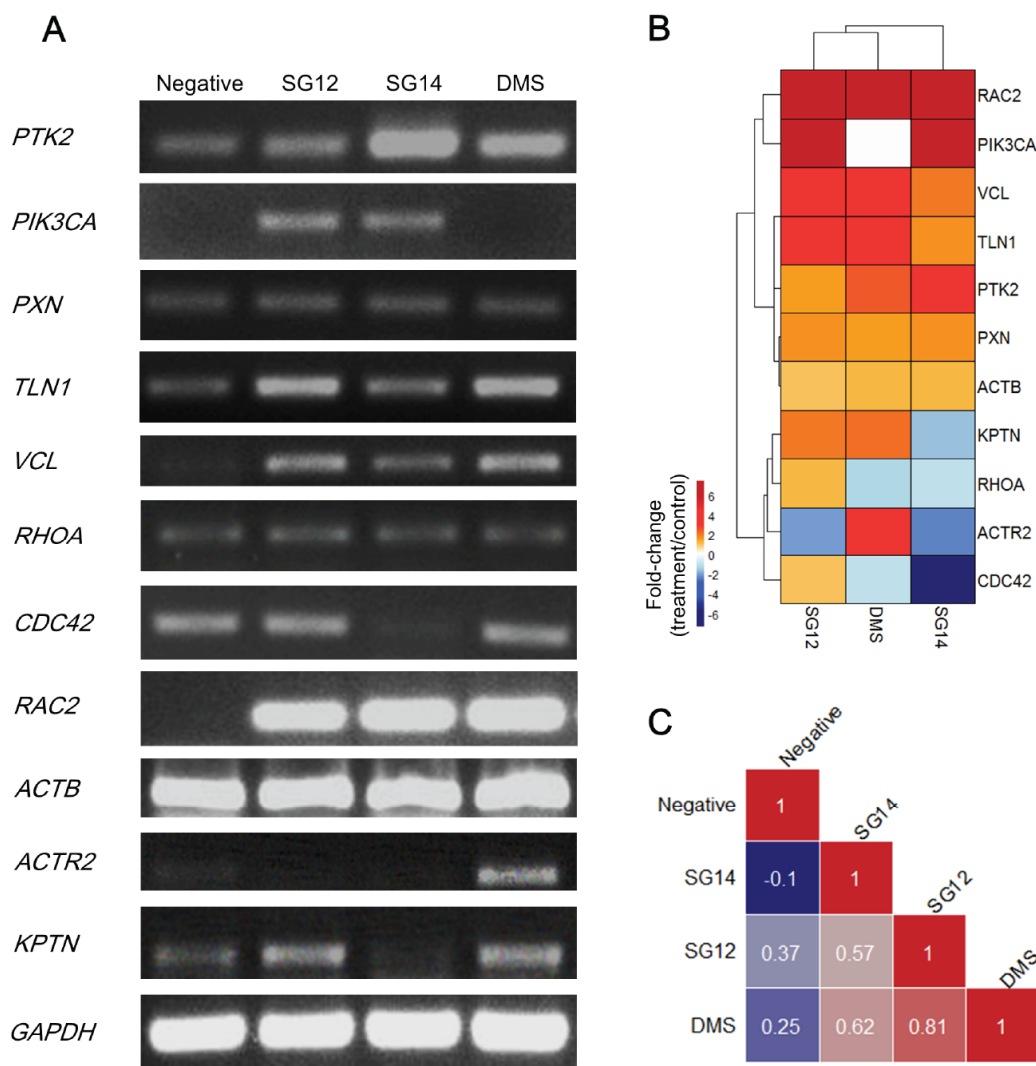


Fig. (4). Expression and heatmap analyses of motility-related genes. (A) The expression levels of *PTK2*, *PIK3CA*, *PXN*, *TLN1*, *VCL*, *RHOA*, *CDC42*, *RAC2*, *ACTB*, *ACTR2*, and *KPTN* with the treatment of the inhibitors. *GAPDH* was used as an internal control. The figure is a representative result from at least 7 independent experiments. (B) Heatmap of motility-related genes. The expression levels were normalized by using *GAPDH* as an internal control, and then each value was normalized against the no treatment control. The clustering columns and rows are shown as lines. (C) Spearman correlation between the inhibitor-treated and untreated samples.

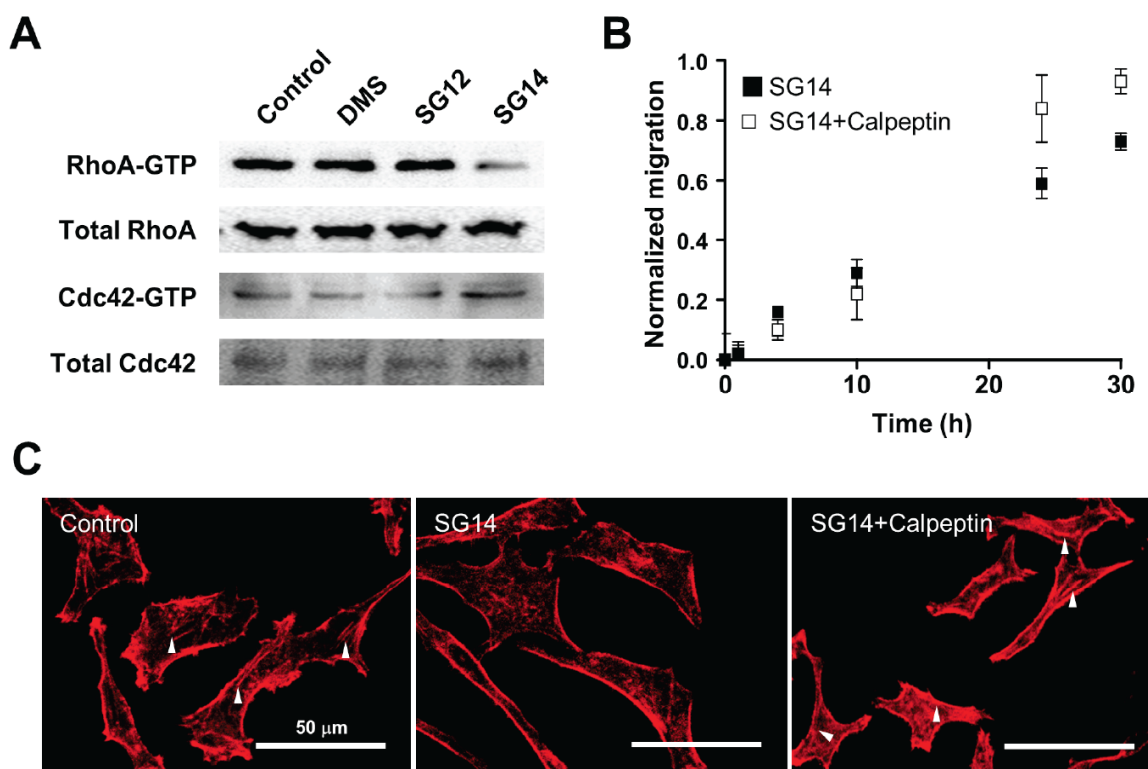


Fig. (5). The effects of SphK2 inhibitors on dynamically regulated proteins. (A) The effects of inhibitors on activation of RhoA and Cdc42 were measured by using pull-down assays. The SG14-treated cells showed a clear decrease in RhoA activation compared with untreated control cells. (B) The effect of a RhoA activator, calpeptin, on SG14-treated cells was studied by monitoring the cumulative migratory behaviors of SG14-treated HeLa cells with or without the treatment of 10 μ M calpeptin in a gap filling assay. The cumulative migration was partially rescued by the addition of calpeptin suggesting that the SG14-mediated retardation of motility was related to RhoA activity. (C) The F-actin cytoskeletal structure of SG14-treated cells with or without the addition of calpeptin were analyzed by confocal microscopy. Arrow heads indicated long F-actin formation. The results showed that the loss of long-F-actin formation upon the treatment of SG14 was partially rescued by the addition of calpeptin. The scale bars indicate 50 μ m.

retardation in cell speed by SG14 is mediated by decreases in stress fibers and long F-actin formation, while the retardation due to SG12 is mediated by nuclear F-actin formation.

3.5. Reverse Transcription PCR

Since the treatment of inhibitors results in differential formation of actin cytoskeletons, we then investigated how each inhibitor modulates the signal transduction pathway involved in the regulation of F-actin, which consequently alters cell motility. Gene expression analyses on motility-related genes (*PTK2*, *PIK3CA*, *PXN*, *TLN1*, *VCL*, *RHOA*, *CDC42*, *RAC2*, *ACTB*, *ACTR2*, and *KPTN*) were performed using HeLa cells treated with SG12, SG14, or DMS via RT-PCR. *GAPDH* was used as an internal control (Fig. 4A). Genes that are up- or down-regulated by more than two-fold are listed in Table 1. The names of the gene products are as follows: *PTK2*, protein tyrosine kinase 2 (PTK2); *PIK3CA*, phosphoinositide-3-kinase (PI3K); *PXN*, paxillin; *TLN1*, talin; *RHOA*, ras homolog family member A (RhoA); *CDC42*, cell division cycle 42 (CDC42); *RAC2*, Ras-related C3 botulinum toxin substrate 2 (Rac2); *ACTB*, actin beta (ACTB); *ACTR2*, actin-related protein 2 (ARP2); and *KPTN*, kaptin [11-21]. Immediate targets of PTK2 are PI3K, paxillin, and talin. Talin regulates vinculin, which in turn affects ACTB, which, at the same time, is affected by CDC42-mediated Rac2 activity. ACTB polymerizes to form actin cytoskeleton, and, finally, F-actin regulates cell motility.

The gene expression study showed that the treatment with SphK2-specific inhibitors turned on the expression of several motility related genes such as *PIK3CA* and *ACTR2* and up-regulated the expression of *RAC2*. The known functions of these

genes are largely related to the PIP₃ signaling and suggest that the inhibition of SphK2 controls the cell motility via altering PIP₃ signaling pathways. While SG12 and SG14 both affected the expressions of PIP₃ related genes, the gene expression patterns of SG12-treated cells were observed to have greater similarity to DMS-treated cells than to SG14-treated cells. Fig. 4A and B show that SG12-treatment induced up-regulation of all genes except for *ACTR2*, compared with the negative control. On the other hand, SG14 treatment up-regulated the expressions of *PTK2*, *PIK3CA*, *PXN*, *TLN1*, *VCL*, and *RAC2*. The expressions of *CDC42*, *ACTR2*, and *KPTN* were absent in this group, and the expression of *PXN*,

Table 1. List of up- or down-regulated genes by the treatment of the inhibitors.

Regulation	SG12	SG14	DMS
Up		<i>PTK2</i>	<i>PTK2</i>
		<i>PIK3CA</i>	<i>PIK3CA</i>
		<i>TLN1</i>	<i>TLN1</i>
		<i>VCL</i>	<i>VCL</i>
		<i>RAC2</i>	<i>RAC2</i>
Down		<i>CDC42</i>	-
		<i>ACTR2</i>	-

RHOA, and *ACTB* were similar to the negative control group. Notably, similar levels of *ACTB* expression were observed in all groups, suggesting that the changes in cytoskeletal structure in inhibitor-treated groups were not due to the decrease in the amount of actin monomers.

We then looked further into the effect of inhibitors on highly dynamic genes, namely *RhoA* and *Cdc42*. As they are major genes involved in dynamic reorganization of actin cytoskeleton. As they are known to be dynamically regulated, we studied the effects after shorter exposure time, 30 min, compared with previous 12 h treatment. First, we measured the RNA expression levels quantitatively after treating with each inhibitor for 30 min by quantitative PCR (Fig. S3). We did not observe any notable changes and this result suggests that the levels of these gene expression is not affected by the inhibitors. We then tried to understand whether inhibitors can alter the dynamic perspectives on the regulation of RhoA and Cdc42 activity. The effects of inhibitors on activation of RhoA and Cdc42 were measured by using pull-down assays (Fig. 5A). The results showed that the amount of activated RhoA proteins (GTP-bound forms) were decreased in SG14-treated cells but DMS- or SG12-treated cells had similar levels compared with control cells. However, the activation of Cdc42 was not altered compared with the control regardless of the inhibitors treated. This result suggests that only SG14 inhibited the activation of RhoA to reduce stress fiber formation, thereby reducing cell motility. The observation also agrees with our data that increasing the concentration of SG14 decreased the formation of stress fibers (data not shown). To confirm that whether the decreased formation of stress fibers and motility in SG14-treated cells were indeed due to diminished activation of RhoA, we exposed SG14-treated cells to a RhoA activator, calpeptin. The stress fiber formation of SG14-treated cells were induced by calpeptin and we observed substantial recovery of cell motility in gap-filling assay (Fig. 5B and 5C). Together, the results suggested that SG14 decreases cell motility by specifically downregulating the activity of RhoA protein.

4. DISCUSSIONS

During cancer progress, some fractions of primary cancer cells acquire the ability to metastasize through multiple genetic alterations [22]. Currently, majority of anti-cancer medications are focused on the inhibition of cancer cell proliferation [23]. However, over 90% of cancer deaths are associated with metastasis. Cell migration is the essential procedure for cancer metastasis but there is no specific anti-metastatic drug available on the market at present. In developing a putative drug candidates for anti-metastasis, it is important to understand how the inhibitors of cell migration control the mobility of cells [24]. Here, we investigated the effects of specific SphK2 inhibitors on cell mobility by monitoring the changes in cumulative and individual motilities, cytoskeletal structures, as well as the expression levels of motility-related genes.

Sphingolipids are important signaling molecules that regulate various cellular functions [25-27]. Interestingly, sphingosines are known to be pro-apoptotic, while the phosphorylation product of sphingosine, S1P, is reported to induce cell proliferation, migration, and survival. As such, the kinases that interconvert sphingolipids are proteins of interest. Among many kinases, we here focused on SphK2, a human enzyme that catalyzes the phosphorylation of sphingosine to S1P, and investigated the effects of SphK2-specific inhibitors, SG12 and SG14, on cell motility in comparison with DMS, a non-specific inhibitor control, which inhibits the functions of both SphK1 and SphK2 as well as protein kinase C. SphK1 and SphK2 share homology and both catalyze the production of S1P, but at different locations in a cell, and thus function in different manners [2]. While their individual functions in cells are not completely elucidated, many reports indicate that SphK2 is tightly related to the cell migration event, thus, a specific inhibitor of

SphK2 may make a good drug candidate, for example, anti-metastasis drug [5].

We first performed MTT assay and gap filling assay to compare the cytotoxicity and the inhibitory effect on cell migration of each inhibitor. Then, the result was further studied by monitoring individual motility parameters and by investigating the changes in cytoskeletal structure and cell morphology as well as by monitoring the changes in the expression levels of motility-related genes. The MTT and gap filling assay demonstrated that SG12 and SG14 are more potent and less cytotoxic inhibitors of cell migration compared with DMS. Since the down-regulation of *ACTR2* expression leads to a retardation in cell motility in other cell types, the absence of *ACTR2* expression in SG12- and SG14-treated cells may be the reason for more efficient inhibition of SG12 and SG14 in cell motility observed in gap filling assays, compared with DMS (Figs. 1B and 4) [28].

The determined motility parameters include trajectory of migration (speed), persistence, direction change, and acceleration. While all three inhibitor-treated cells commonly showed significant decreases in trajectories of migration compared with negative control cells, other motility parameters responded in specific manners depending on the inhibitors treated. Further studies indicated that the mechanisms of inhibition were rather different between SG12 and SG14. There are several observations supporting this hypothesis. First, the stress fiber formation is greatly reduced in SG14-treated cells, which are involved in contraction during migration (Fig. 3A). The notion was supported by 1) treating cells with higher concentrations of SG14 further reduced stress fiber formation 2) only SG14 decreases the level of activated RhoA (Fig. 5A) and 3) the addition of a Rho activator (calpeptin) partially restored the stress fiber formation in SG14-treated cells (Fig. 5B and 5C). Second, SG12-treated cells showed nuclear F-actin staining. Generally, cells that have nuclear F-actin are spread out and become less motile. This also corresponds with the previous report that SphK2 is predominantly localized to the nucleus and plays a role in HDAC activity which is linked to cell motility [29]. Inhibition of HDAC activity also leads to the inhibition of cell motility and invasion in prostate cancer cells [30]. Third, SG14-treated cells showed less persistent movement compared with SG12-treated cells. Unlike other groups, extensive formation of lamellipodial F-actin right below the ruffled edge was not observed in SG14-treated cells, as indicated by open arrowheads in Fig. 3A. This may be due to the loss of *KPTN* expression, which is involved with the initiation of F-actin formation at the leading edge [31, 32]. In addition, SG14-treated cells showed absence of *CDC42* RNA and protein expression (Figs. 4A and 5A), which is involved with controlling the direction of cell migration and the formation of filopodia [33]. Finally, RT-PCR analysis showed that *PTK2* was pronouncedly up-regulated in SG14-treated cells. *PTK2* encodes focal adhesion kinase which serves as anchorage device that maintains the cell morphology in stationary cells, thereby keeping the cells from being highly motile [34].

To summarize, SG12 and SG14 affect cell motility *via* altering the expression levels of different genes involved in cell migration. Many of these genes are related to actin polymerization, which, in turn, modulates motility parameters in specific manners with a net effect of decreased cumulative cell motility, as shown by gap filling assay.

CONCLUSION

We confirmed that the SphK2-specific inhibitors, SG12 and SG14, inhibited the migration of cancerous human cell line, HeLa, more effectively compared with the non-specific inhibitor, DMS, at a low concentration of inhibitors. We also showed that the mode of inhibition was different between SG12, SG14, and DMS through the analysis of motility parameters, the expression of motility-

related genes, activated RhoA pull-down assay, and RhoA activation assay. Since abnormal migration is one of the most propounding features of cancer metastasis, the results suggest that the anti-migratory effect of SphK2-specific inhibitors may make them optimal candidates for novel anti-metastatic agents.

CONFLICT OF INTEREST

The authors declare that there is no conflict of interest regarding the publication of this paper.

ACKNOWLEDGEMENTS

The authors gratefully acknowledge the financial support from the Korea Ministry of Science, ICT & Future Planning (MSIP) (Grant No. 2014043300032, Basic Research Program) and National Research Foundation of Korea (NRF) (Grant No. 20110009969, Basic Research Program).

SUPPLEMENTARY MATERIAL

Supplementary material is available on the publisher's web site along with the published article.

REFERENCES

- [1] Qin, Z.; Dai, L.; Trillo-Tinoco, J.; Senkal, C.; Wang, W.; Reske, T.; Bonstaff, K.; Del Valle, L.; Rodriguez, P.; Flemington, E.; Voelkel-Johnson, C.; Smith, C.D.; Ogretmen, B.; Parsons, C., Targeting sphingosine kinase induces apoptosis and tumor regression for KSHV-associated primary effusion lymphoma. *Mol. Cancer Ther.*, **2014**, *13* (1), 154-164.
- [2] Pitson, S.M., Regulation of sphingosine kinase and sphingolipid signaling. *Trends Biochem. Sci.*, **2011**, *36* (2), 97-107.
- [3] Yotsumoto, F.; Tokunaga, E.; Oki, E.; Maehara, Y.; Yamada, H.; Nakajima, K.; Nam, S.O.; Miyata, K.; Koyanagi, M.; Doi, K.; Shirasawa, S.; Kuroki, M.; Miyamoto, S., Molecular hierarchy of heparin-binding EGF-like growth factor-regulated angiogenesis in triple-negative breast cancer. *Mol. Cancer Res.*, **2013**, *11* (5), 506-517.
- [4] Kim, J.W.; Kim, Y.W.; Inagaki, Y.; Hwang, Y.A.; Mitsutake, S.; Ryu, Y.W.; Lee, W.K.; Ha, H.J.; Park, C.S.; Igarashi, Y., Synthesis and evaluation of sphingoid analogs as inhibitors of sphingosine kinases. *Bioorg. Med. Chem.*, **2005**, *13* (10), 3475-385.
- [5] Wong, L.; Tan, S.S.L.; Lam, Y.; Melendez, A.J., Synthesis and Evaluation of Sphingosine Analogues as Inhibitors of Sphingosine Kinases. *J. Med. Chem.*, **2009**, *52* (12), 3618-3626.
- [6] Prewitt, J. M.; Mendelsohn, M. L., The analysis of cell images. *Ann. N. Y. Acad. Sci.*, **1966**, *128* (3), 1035-1053.
- [7] Steger, C., An Unbiased Detector of Curvilinear Structures. *IEEE Trans. Pattern Anal. Mach. Intell.*, **1998**, *20* (2), 113-125.
- [8] Anon, E.; Serra-Picamal, X.; Hersen, P.; Gauthier, N. C.; Sheetz, M. P.; Treppe, X.; Ladoux, B. T., Cell crawling mediates collective cell migration to close undamaged epithelial gaps. *Pro. Natl. Acad. Sci.*, **2012**, *109* (27), 10891-10896.
- [9] Vallenius, T., Actin stress fibre subtypes in mesenchymal-migrating cells. *Open Biol.*, **2013**, *3* (6), 130001.
- [10] Plessner, M.; Melak, M.; Chinchilla, P.; Baarlink, C.; Grosse, R., Nuclear F-actin formation and reorganization upon cell spreading. *J. Biol. Chem.*, **2015**, *290* (18), 11209-11216.
- [11] Schaller, M.D., Cellular functions of FAK kinases: insight into molecular mechanisms and novel functions. *J. Cell. Sci.*, **2010**, *123* (7), 1007-1013.
- [12] Yamaguchi, H.; Yoshida, S.; Muroi, E.; Yoshida, N.; Kawamura, M.; Kouchi, Z.; Nakamura, Y.; Sakai, R.; Fukami, K., Phosphoinositide 3-kinase signaling pathway mediated by p110alpha regulates invadopodia formation. *J. Cell Biol.*, **2011**, *193* (7), 1275-1288.
- [13] Ma, Y.Y.; Wei, S.J.; Lin, Y.C.; Lung, J.C.; Chang, T.C.; Whang-Peng, J.; Liu, J.M.; Yang, D.M.; Yang, W.K.; Shen, C.Y., PIK3CA as an oncogene in cervical cancer. *Oncogene*, **2000**, *19* (23), 2739-2744.
- [14] Mazaki, Y.; Hashimoto, S.; Sabe, H., Monocyte cells and cancer cells express novel paxillin isoforms with different binding properties to focal adhesion proteins. *J. Biol. Chem.*, **1997**, *272* (11), 7437-7444.
- [15] Xu, W.; Baribault, H.; Adamson, E.D., Vinculin knockout results in heart and brain defects during embryonic development. *Development*, **1998**, *125* (2), 327-337.
- [16] Tapon, N.; Hall, A., Rho, Rac and Cdc42 GTPases regulate the organization of the actin cytoskeleton. *Curr. Opin. Cell Biol.*, **1997**, *9* (1), 86-92.
- [17] Chrzanoska-Wodnicka, M.; Burridge, K., Rho-stimulated contractility drives the formation of stress fibers and focal adhesions. *J. Cell Biol.*, **1996**, *133* (6), 1403-1415.
- [18] Luckashenak, N.; Wahe, A.; Breit, K.; Brakebusch, C.; Brouck, T., Rho-family GTPase Cdc42 controls migration of Langerhans cells *in vivo*. *J. Immunol.*, **2013**, *190* (1), 27-35.
- [19] Ridley, A.J., Rho GTPases and actin dynamics in membrane protrusions and vesicle trafficking. *Trends Cell Biol.*, **2006**, *16* (10), 522-529.
- [20] Ballestrem, C.; Wehrle-Haller, B.; Hinz, B.; Imhof, B.A., Actin-dependent Lamellipodia Formation and Microtubule-dependent Tail Retraction Control-directed Cell Migration. *Mol. Biol. Cell*, **2000**, *11* (9), 2999-3012.
- [21] Liu J.; Zou, L.; Wang, J.; Zhao, Z., Validation of beta-actin used as endogenous control for gene expression analysis in mechanobiology studies. *Stem Cells*, **2009**, *27* (9), 2371-2372.
- [22] Yokota, J., Tumor progression and metastasis. *Carcinogenesis*, **2000**, *21* (3), 497-503.
- [23] Weber, G.F., Why does cancer therapy lack effective anti-metastasis drugs? *Cancer Lett.*, **2013**, *328* (2), 207-211.
- [24] Stock, A.M.; Troost, G.; Niggemann, B.; Zanker, K.S.; Entschladen, F., Targets for anti-metastatic drug development. *Curr. Pharm. Des.*, **2013**, *19* (28), 5127-5134.
- [25] Hannun, Y.A.; Obeid, L.M., Mechanisms of Ceramide-Mediated Apoptosis in: Eicosanoids and other Bioactive Lipids in Cancer, Inflammation, and Radiation Injury 3, Honn, K.V.; Marnett, L.J.; Nigam, S.; Jones, R.L.; Wong, P.Y.K., Eds. Springer US: Boston, MA, **1997**; 145-149.
- [26] Hannun, Y.A.; Obeid, L.M., Principles of bioactive lipid signalling: lessons from sphingolipids. *Nat. Rev. Mol. Cell Biol.*, **2008**, *9* (2), 139-150.
- [27] Zhang, H.; Desai, N.N.; Olivera, A.; Seki, T.; Brooker, G.; Spiegel, S., Sphingosine-1-phosphate, a novel lipid, involved in cellular proliferation. *J. Cell Biol.*, **1991**, *114* (1), 155-167.
- [28] Machesky, L.M.; Gould, K.L., The Arp2/3 complex: a multifunctional actin organizer. *Curr. Opin. Cell Biol.*, **1999**, *11* (1), 117-121.
- [29] Hait, N.C.; Allegood, J.; Maceyka, M.; Strub, G.M.; Harikumar, K.B.; Singh, S.K.; Luo, C.; Marmorstein, R.; Kordula, T.; Milstien, S.; Spiegel, S., Regulation of histone acetylation in the nucleus by sphingosine-1-phosphate. *Science*, **2009**, *325* (5945), 1254-1257.
- [30] Kim, N.H.; Kim, S.N.; Kim, Y.K., Involvement of HDAC1 in E-cadherin expression in prostate cancer cells; its implication for cell motility and invasion. *Biochem. Biophys. Res. Commun.*, **2011**, *404* (4), 915-921.
- [31] Bearer, E.L.; Abraham, M.T., 2E4 (kaptin): a novel actin-associated protein from human blood platelets found in lamellipodia and the tips of the stereocilia of the inner ear. *Eur. J. Cell Biol.*, **1999**, *78* (2), 117-126.
- [32] Bearer, E.L., Role of actin polymerization in cell locomotion: molecules and models. *Am. J. Resp. Cell Mol. Biol.*, **1993**, *8* (6), 582-591.
- [33] Nobes, C.D.; Hall, A., Rho, rac, and cdc42 GTPases regulate the assembly of multimolecular focal complexes associated with actin stress fibers, lamellipodia, and filopodia. *Cell*, **1995**, *81* (1), 53-62.
- [34] Morgan, M.R.; Humphries, M.J.; Bass, M.D., Synergistic control of cell adhesion by integrins and syndecans. *Nat. Rev. Mol. Cell Biol.*, **2007**, *8* (12), 957-969.